Chinese Journal of
POLYMER SCIENCE

RESEARCH ARTICLE

https://doi.org/10.1007/s10118-022-2798-x
Chinese J. Polym. Sci. **2022**, *40*, 1101–1109

An ROS-Responsive Antioxidative Macromolecular Prodrug of Caffeate for Uveitis Treatment

Yu-Tong Li[a,†], Si-Ting Sheng[b,†], Bo Yu[a], Fan Jia[a], Kai Wang[b*], Hai-Jie Han[b], Qiao Jin[a], You-Xiang Wang[a], and Jian Ji[a*]

[a] *MOE Key Laboratory of Macromolecule Synthesis and Functionalization of Ministry of Education, Department of Polymer Science and Engineering, Zhejiang University, Hangzhou 310027, China*
[b] *Eye Center, the Second Affiliated Hospital, School of Medicine, Zhejiang University, Hangzhou 310009, China*

Electronic Supplementary Information

Abstract Uveitis is a sophisticated syndrome showing a high relevance with reactive oxygen species (ROS). Herein, an ROS-responsive PEGylated polypeptide based macromolecular prodrug of herbaceous antioxidant ethyl caffeate (EC) is designed *via* phenylboronic esters with improved solubility for the alleviation of uveitis. The antioxidative 4-hydroxybenzyl alcohol (HBA) and EC can be released from the macromolecular EC prodrug under the stimulation of ROS, which can effectively protect cells against oxidative stress-induced injury in an ROS-depletion way. The antioxidative and protective effects of the macromolecular EC prodrug *in vivo* are further verified in a uveitis mouse model. Overall, this work not only provides a handy method to synthesize a phenylboronic ester-bearing EC prodrug which is highly sensitive to pathological ROS, but also depicts a promising future to apply macromolecular antioxidative prodrugs in the treatment of uveitis as well as other ROS-related diseases.

Keywords Antioxidative therapy; Macromolecular prodrug; Uveitis; Ethyl caffeate (EC); Phenylboronic acid esters

Citation: Li, Y. T.; Sheng, S. T.; Yu, B.; Jia, F.; Wang, K.; Han, H. J.; Jin, Q.; Wang, Y. X.; Ji, J. An ROS-responsive antioxidative macromolecular prodrug of caffeate for uveitis treatment. *Chinese J. Polym. Sci.* **2022**, *40*, 1101–1109.

INTRODUCTION

Uveitis is a complex ocular inflammation of uvea, including iris, ciliary body as well as chorioidea, and adjacent apparatus like retina, optic nerves, vitreum even sclera may get affected at the same time.[1–3] It was reported that 5%–10% of the visual impairment, along with 10%–15% of blindness was caused by uveitis around the world,[4] which would be much more severe in developing countries.[5] There are many reasons to cause uveitis. However, compared with infection-induced uveitis, which could be mitigated by anti-infective therapy, aseptic uveitis is much more challenging to deal with for its sophisticated inducement such as immune dysfunction and autoinflammatory response.[4] An increasing number of studies pointed out that the imbalance of reactive oxidant species (ROS) played a vital role in numerous kinds of inflammation, including uveitis.[6] As a typical proinflammatory mediator, ROS bears a great potential to propagate the formation of inflammasomes and promote the secretion of inflammatory mediators like interleukin (IL)-1β and IL-18.[7–12] On the other hand, the excessive ROS, or so-called oxidative stress, will oxidate and destroy lipids and proteins in normal cells, thus poses a great threat in affected tissues.[13,14]

Considering the essential role of ROS in the progression of inflammatory diseases, more and more attempts have been reported to introduce antioxidants for the alleviation of inflammatory diseases including uveitis.[15–18] As an herbaceous antioxidant, ethyl caffeate (EC) is widely applied in anti-inflammatory and anti-infectious areas.[19–21] However, the bioavailability and therapeutic efficiency of EC are severely limited due to its low water solubility. To break this constriction, a macromolecular prodrug strategy is very promising for its improvement of solubility.[22,23] Polypeptides are ideal macromolecular carriers with many advantages, such as easy synthesis and functionalization, excellent solubility, biocompatibility and degradability.[24–26]

The "smart delivery" is usually referred in the rational design of drug delivery systems which requires the site-specific release of drugs in the pathological microenvironment (acidic pH, specific enzymes, redox, *etc.*), which is generally significantly different to that of normal tissue.[27–31] Technically, the high ROS level in uveitis itself could be utilized as a

* Corresponding authors, E-mail: kaiwang94@zju.edu.cn (K.W.)
E-mail: jijian@zju.edu.cn (J.J.)
† These authors contributed equally to this work.
Special Issue: Biomedical Polymers
Received April 15, 2022; Accepted May 26, 2022; Published online July 12, 2022

trigger.[32,33] Because of the responsiveness to high ROS level, phenylboronic acid esters are attracting a great deal of attention for the design of stimuli-responsive drug delivery systems.[34] Interestingly, it is reported that an ROS scavenger 4-hydroxybenzyl alcohol (HBA) can be produced as a byproduct during the releasing process when 4-hydroxymethyl phenylboronic acid is used to prepare phenylboronic acid esters.[35] Therefore, such 4-hydroxymethyl phenylboronic acid ester is especially promising in antioxidative and anti-inflammatory applications.

Herein, a PEGylated polypeptide based macromolecular prodrug of EC was developed for the treatment of aseptic uveitis. The macromolecular EC prodrug (P-HPEC) was synthesized by conjugating 4-(hydroxymethyl) phenylboronic acid ethyl caffeate ester (HPEC) to the side chains of ethanolamine modified PEG-*b*-polyglutamic acid (P-OH) (Fig. 1A). The prepared prodrug P-HPEC could be easily dissolved in water. Meanwhile, EC and HBA could be effectively released in the high ROS level microenvironment of aseptic uveitis. The ROS scavenging ability of P-HPEC was inherited from the released EC and HBA. Accordingly, P-HPEC could protect L929 fibroblasts and human corneal epithelial cells (HCEC) due to the decrease of oxidative stress, which was much more effective than the free drugs. The excellent antioxidative capability of P-HPEC was further confirmed *in vivo* by a uveitis mouse model. Therefore, an ROS-responsive EC prodrug with high water solubility was designed. The antioxidative capacity of EC was enhanced with the help of HBA, leading to a superior therapeutic outcome against uveitis in an ROS-scavenging manner.

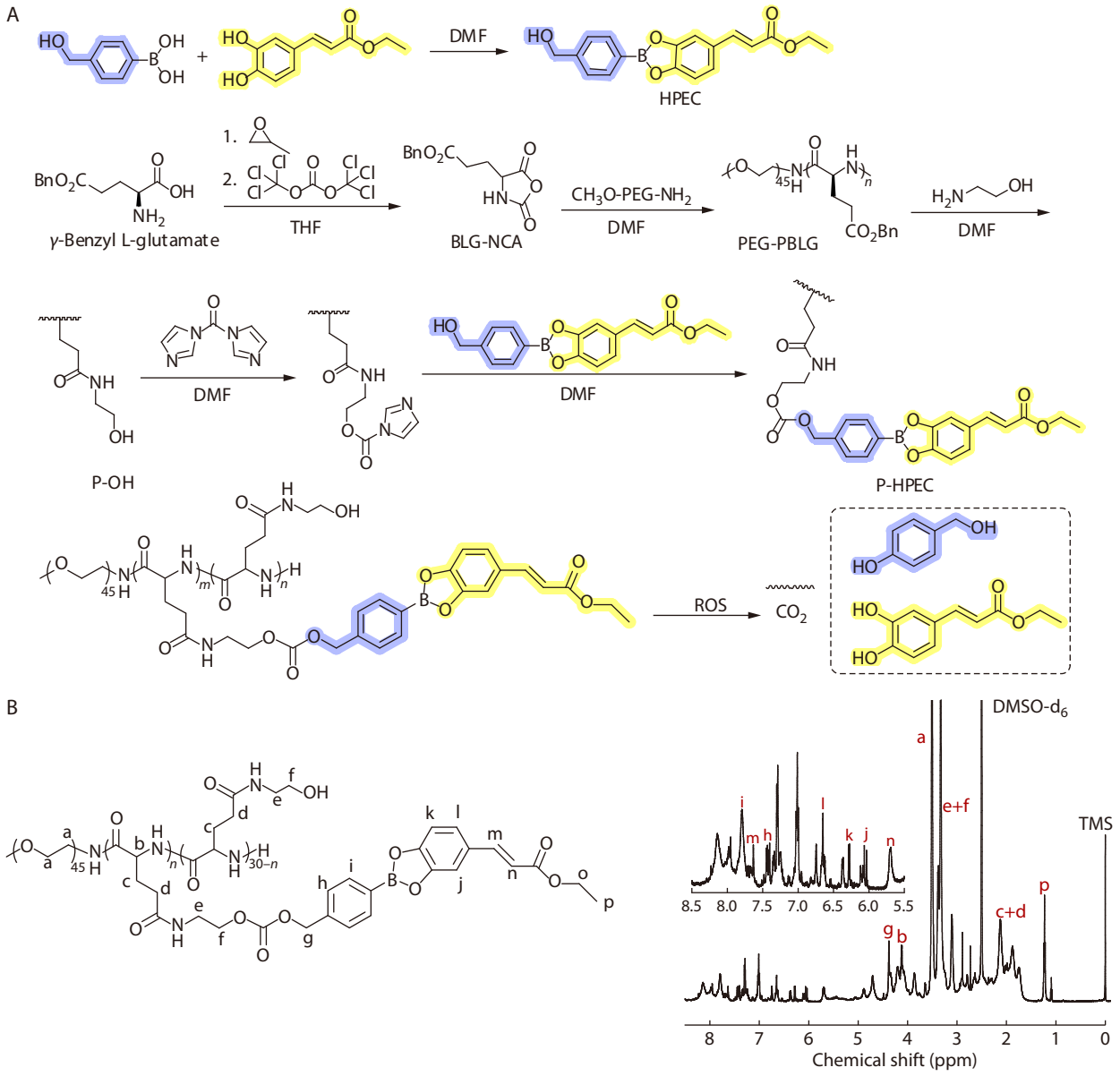

Fig. 1 Synthesis and characterization of macromolecular EC prodrug P-HPEC. (A) Synthetic route of P-HPEC and its mechanism of scavenging ROS; (B) ^{1}H-NMR spectrum of P-HPEC in DMSO-d_6.

MATERIALS AND METHODS

Materials and Characterizations

DMF, ethyl acetate, THF, NaCl, anhydrous Na_2SO_4, hexane, ether, acetonitrile, DMSO, H_2O_2 and ethanol were purchased from Sinopharm Chemical Reagent Co., Ltd. (Shanghai, China). EC, 4-hydroxymethyl phenylboric acid, γ-benzyl L-glutamate, 2-hydroxypyridine and ethanolamine were purchased from Energy Chemical Co., Ltd. (Shanghai, China). Methyloxirane and LiBr were obtained from TCI (Shanghai) Development Co., Ltd. (Shanghai, China). Triphosgene, 1,1'-carbonyldiimidazole, anhydrous DMF and methoxypolyethylene glycol amine were brought from Macklin Inc. (Shanghai, China). CD_3OD, DMSO-d_6, DAPI and lipopolysaccharide (LPS) were brought from Sigma-Aldrich (St. Louis, MO, USA). $CDCl_3$ was purchased from Adamas Reagent, Ltd. DPPH was supplied by TargetMol Chemicals Inc. (Boston, MA). 4-Dimethylaminopyridine, Rhodamine B and paraformaldehyde were purchased from Aladdin Biochemical Technology Co., Ltd. (Shanghai, China). Roswell Park Memorial Institute (RPMI) 1640 medium, Dulbecco's modified Eagle's medium and Ham's F12 medium (DMEM/F12) and Penicillin-Streptomycin were provided by Cienry Ltd. (Huzhou, China). Fetal bovine serum (FBS), RIPA buffer, Halt™ Protease Inhibitor Cocktail, EDTA-Free (100×), SuperSignal West Dura Extended Duration Substrate, Goat anti-Rabbit IgG (H+L) (HRP labelled) and Goat anti-Mouse IgG (H+L) (HRP labelled) secondary antibodies were obtained from Thermo Fisher Scientific Inc. (Waltham, MA). Cell Counting Kit-8 (CCK-8) was supplied by Dalian Meilun Biotechnology Ltd. (Dalian, China). 20×PBS buffer was bought from Sangon Biotech. Co., Ltd. (Shanghai, China). Reactive Oxygen Species Assay Kit (DHE) was purchased from Bestbio Co., Ltd. (Shanghai, China). BCA Protein Assay Kit was purchased from Beyotime Institute of Biotechnology (Haimen, China). Acrylamide Solution (30%) was obtained from Bio-Rad Laboratories, Inc. (Hercules, California, USA). BSA was supplied by Sangon Biotech (Shanghai) Co., Ltd. (Shanghai, China). X-ray film was purchased from Huadong Medicine Co., Ltd. (Hangzhou, China). TNF-α, Nrf2, HO-1 and β-actin primary antibodies were purchased from Abcam plc (Cambridge, UK). ECL DualVue WB Marker was purchased from General Electric Company (Boston, USA).

The chemical structure or average molecular weight of prepared prodrug and its precursors were analysed by ^{1}H-NMR, using a Bruker AVANCE III 500 MHz spectrometer. The number- (M_n) or weight- (M_w) average molecular weight as well as the polymer dispersity index (PDI) of PEG-PBLG and P-OH were measured with GPC (Waters 1515/2414). The mobile phase was LiBr/DMF with a flow rate of 1 mL/min and the injection volume was 50 μL of stock solution (4.5 mg of PEG-PBLG or P-OH dissolved in 1.5 mL of LiBr/DMF), using monodisperse polystyrene as a standard. UV-Vis spectrophotometer (SHIMADZU UV-2550) was carried out in the wavelength range of 200–600 nm to assess the spectra of prepared prodrug and its precursors. Cell viability was determined by an Agilent BioTek Synergy H1 Multimode Reader. Fluorescent images of cell uptake or intracellular ROS were captured under a Nikon Eclipse Ts2 Inverted Routine Microscope. Protein blots in western blot analysis were visualized by chemiluminescence (ChemiScope 6100).

Synthesis of Macromolecular EC Prodrug P-HPEC

Synthesis of HPEC

EC (1.87 g, 9 mmol) and 4-hydroxymethyl phenylboric acid (1.38 g, 10 mmol), dissolved in 10 mL of DMF, were stirred at 100 °C for 8 h, and the mixture gradually turned to a clear, dark green color during the reaction. The solvent was removed by rotary evaporation until the substance in the reaction vessel became an atrovirens tar. 5 mL of cold ethyl acetate (−20 °C) was poured into the concentrate and the mixture was stored overnight at −20 °C for recrystallization. The precipitated white powder was collected and dried in vacuum at room temperature to obtain the product. (Methanol-d_4 for ^{1}H-NMR).

Synthesis of γ-benzyl L-glutamate N-carboxyanhydrides (BLG-NCA)

After blending γ-benzyl L-glutamate (5.0 g, 21.1 mmol, 1.0 equiv.), THF (75 mL) and methyloxirane (6.5 mL, 84.5 mmol, 4.0 equiv.) under magnetic stirring, triphosgene (3.15 g, 10.6 mmol, 0.5 equiv.) was added and the reaction vessel was immediately sealed. When the turbid solution was clarified after reaction for 2 h, for safety reasons, 35 mL of deionized water was added to the mixture to react with excessive triphosgene for 3 min. The solution was extracted with ethyl acetate (EA, 25 mL × 2), and the combined organic phase was washed twice with saturated salt water and dried with anhydrous Na_2SO_4. The solvent was removed by rotary evaporation at 45 °C; later, the white acicular crystalline products were obtained by recrystallization below 10 °C in hexane or THF.[36] ($CDCl_3$ for ^{1}H-NMR)

Synthesis of PEG-b-polybenzyl L-glutamate (PEG-PBLG)

The initiator methoxypolyethylene glycol amine (203 mg, 0.10 mmol, 1.0 equiv.), dissolved in 1 mL of anhydrous DMF, was quickly added to the solution of BLG-NCA (800 mg, 3.0 mmol, 30 equiv.) in anhydrous DMF (1 mL). The mixture was stirred at 45 °C for 48 h under water-free and oxygen-free condition. Then the mixture was precipitated in excessive ether and centrifuged. The collected product was washed twice with ether and dried overnight in vacuum to obtain the white solid product PEG-PBLG. (DMSO-d_6 for ^{1}H-NMR)

Synthesis of P-OH

PEG-PBLG (150 mg, with ~0.525 mmol grafting benzyloxycarbonyl groups), 2-hydroxypyridine (499.4 mg, 5.25 mmol) and ethanolamine (641.4 mg, 10.5 mmol) were fully mixed in 4 mL of DMF and stirred at 45 °C for 48 h. The solution was then precipitated in a precipitant (acetonitrile:ether=1:1, *V*:*V*). The product was centrifuged, washed with ether for twice and dried overnight in vacuum, which finally was yellowish brown and slightly viscous solid. (DMSO-d_6 for ^{1}H-NMR)

Synthesis of P-HPEC

P-OH (100 mg, with ~0.42 mmol grafting hydroxyl group) and 1,1'-carbonyldiimidazole (CDI, 135.8 mg, 0.84 mmol) were dissolved in 8 mL of DMF and reacted under stirring at 45 °C for 6 h. Then, deionized water, equivalent to CDI, was added under agitation to prevent unreacted CDI from precipitation in the subsequent process. After 4-dimethylaminopyridine (DMAP, 51.1 mg, 0.42 mmol) and the solution of HPEC (298.3 mg, 0.84 mmol) in 4 mL DMF were added to the reaction vessel, the mixture was stirred at 45 °C for 72 h in the dark, and then precipitated in excessive ether. The solid product was collected by centrifugation and washed for twice with ether. Our

https://doi.org/10.1007/s10118-022-2798-x

macromolecular EC prodrug P-HPEC was ultimately obtained as olive-drab powder after vacuum drying overnight. (DMSO-d_6 for ^{1}H-NMR)

In vitro Release of P-HPEC

In vitro release study, PBS (pH=7.4) with or without 1.0 mmol/L H_2O_2 was used as the release medium to investigate the release of P-HPEC in it. Briefly, 1 mL of solution of P-HPEC in PBS containing 0.5 mg of P-HPEC was sealed into a dialysis membrane (MWCO 1kDa)-sealed chamber and immersed into 10 mL PBS or PBS containing 1 mmol/L H_2O_2 in a 37 °C shaker for the period of release *in vitro*. At the preset time points, 300 μL of release medium was collected for measurement, followed by replenishing the same volume of fresh release medium. The released concentration of byproduct HBA in peripheric buffer was quantified by UV-Vis spectrophotometer at 273 nm.

Radical Scavenging Ability of P-HPEC

25 μL of EC with different concentrations (finally ranging from 1.50, 3.75, 7.50, 11.3 to 15.0 μg/mL after mixture) or P-HPEC (with a series of EC of equivalent concentrations) were mixed with 75 μL freshly prepared DPPH solution (100 μmol/L in ethanol) in the shaker at 37 °C for 30 min in the dark to evaluate the ability of P-HPEC to eliminate free radical. Thereafter, absorbance at 517 nm was detected and the relative DPPH concentration was calculated as below:

$$\text{Relative DPPH concentration (\%)} = \frac{A_S - A_B}{A_0 - A_B} \times 100\% \quad (1)$$

where A_S is absorbance of tested samples, A_B is average absorbance of 25 μL of deionized water and 75 μL of ethanol, A_0 is average absorbance of 25 μL of deionized water and 75 μL of DPPH solution in ethanol.

Cell Culture

L929 fibroblasts and human corneal epithelial cells (HCEC) were provided by American Tissue Culture Collection (Manassas, VA, USA). L929 cells were cultured in Roswell Park Memorial Institute (RPMI) 1640 medium with 10% fetal bovine serum (FBS); HCEC were cultured in Dulbecco's modified Eagle's medium and Ham's F12 medium (DMEM/F12) containing 10% FBS and 1% Penicillin-Streptomycin. They were all incubated at 37 °C in a constant temperature incubator with 5% CO_2.

Cell Uptake

P-HPEC (10 mg) and Rhodamine B (1%) were suspended in DMSO at room temperature in the dark for 24 h. The mixture was dialyzed (MWCO 2.5 kDa) against deionized water and freeze dried to get Rhodamine B labelled P-HPEC as pink powder. Rhodamine B labelled P-HPEC (3 mg) was dissolved in 1 mL of PBS to prepare the stock solution. L929 cells were planted in 24-well plates at a density of 3×10^4 cells per well and cultured in an incubator for 24 h to make the cells adhere to the wall. After the removal of medium, the cells were incubated with phenol red-free and serum-free RPMI 1640 containing 20 μL of stock solution for 2, 4 and 6 h, respectively. After incubation for different periods of time, cells were fixed with 500 μL of 4% paraformaldehyde in each well for 15–20 min. Then the cells were rinsed with PBS for 3 times before adding 200 μL of DAPI (1 μg/mL) to restain the nucleus for 10 min. Again, the cells were washed with PBS for 3 times, and 200 μL of PBS was added. The internalization images of Rhodamine B labeled P-HPEC were captured under fluorescence microscope.

Cytotoxicity

CCK-8 assay was used to determine the cell viability of L929 and HCEC after being exposed to a series of prodrug concentrations to evaluate the cytotoxicity of P-HPEC. In brief, 200 μL of medium containing 1×10^4 cells was added to sterile 96-well plates and cultured in an incubator containing 5% CO_2 at 37 °C for 24 h to make cells adherent. Then the medium was sucked out, and 200 μL of medium containing different concentrations of P-HPEC (with a series of equivalent EC concentrations ranging from 1.5 μg/mL to 15 μg/mL) was added to each well. A group without the adding of prodrug under the same conditions was used as control. After incubation for 24 h, the medium was removed and 100 μL of CCK-8 solution was added to each well, followed by another 2 h of incubation. 100 μL of CCK-8 solution was used as blank. Thereafter, the absorbance of each well at 450 nm was measured by a microplate reader and cell viability was calculated as below:

$$\text{Cell viability (\%)} = \frac{A_S - A_B}{A_0 - A_B} \times 100\% \quad (2)$$

where A_S is absorbance of tested samples, A_B is average absorbance of blank, A_0 is average absorbance of control.

Rescuing Ability against Oxidative Stress

To evaluate the rescuing ability against oxidative stress, CCK-8 assay was used to measure the cell viability of L929 and HCEC after exposure to H_2O_2 and simultaneously to different treatments including PBS, EC, P-OH and P-HPEC. Similar to cytotoxicity assay, cells were seeded in 96-well plates at the density of 1×10^4 cells/well and incubated at 37 °C in air containing 5% CO_2 for 24 h. Each experimental group was dosed with H_2O_2 at a final concentration of 50 μmol/L (L929) or 400 μmol/L (HCEC) and simultaneously treated with PBS, EC (7.5 μg/mL), P-HPEC (with an equivalent EC concentration), P-OH (with an equivalent polymer backbone concentration). Cells without being manipulated were used as control. After incubation for 24 h, 100 μL of CCK-8 solution was added to each well, followed by incubation for another 2 h. 100 μL of CCK-8 solution was used as blank. The absorbance at 450 nm of each well was recorded by a microplate reader. Finally, cell viability was calculated as the following equation:

$$\text{Cell viability (\%)} = \frac{A_S - A_B}{A_0 - A_B} \times 100\% \quad (3)$$

where A_S is absorbance of tested samples, A_B is average absorbance of blank, A_0 is average absorbance of control.

Fluorescent Staining of Intracellular ROS

L929 cells were seeded in a 24-well plate at the density of 5×10^4 cells/well and cultured in incubator with 5% CO_2 at 37 °C for 24 h. Thereafter, the medium was changed to phenol red-free and serum-free RPMI 1640 and each experimental group was dosed with H_2O_2 at a final concentration of 50 μmol/L and simultaneously treated with PBS, EC (7.5 μg/mL), P-HPEC (with an equivalent EC concentration), P-OH (with an equivalent polymer backbone concentration). Cells without being manipulated were used as control. After 4 hours' culture, 200 μL of solution of DHE (1:1000 diluted to phenol red-free and serum-free RPMI 1640) was add to each well and the cells were incubated for 40 min. Then the cells were washed with PBS for 3 times and fixed with 500 μL of 4% paraformaldehyde in each well for 15–20 min. After washing with PBS for three times

https://doi.org/10.1007/s10118-022-2798-x

again, 200 μL of PBS was added to each well. The ROS fluorescent images were captured under fluorescence microscope.

Western Blot Analysis

Western blot analysis was conducted to evaluate the *in vitro* anti-inflammatory activity and the ability to resist oxidative stress damage of P-HPEC. L929 cells were seeded into a 6-well plate at the density of 5×10^5 cells/well and cultured in incubator with 5% CO_2 at 37 °C for 24 h. Subsequently, each experimental group was dosed with H_2O_2 at a final concentration of 50 μmol/L and treated with PBS, EC (7.5 μg/mL), P-HPEC (with an equivalent EC concentration), P-OH (with an equivalent polymer backbone concentration), respectively, at the same time. Cells without being manipulated under the same condition were used as control. After incubation for 24 h, cells were lysed with RIPA lysis buffer and the homogenate of each group was collected and centrifuged for supernatant. Protein concentrations were determined by a BCA Protein Assay Kit and the loading volume of each sample was calculated according to its protein loading amount (60 μg). After denaturation, the proteins were separated on a gel plate by electrophoresis and transferred to a poly(vinylidene fluoride) (PVDF) membrane (Millipore), which was then blocked in 5% BSA in TBS with tween 80 at room temperature for 2–3 h. The membranes were incubated with TNF-*α* (1:2000 dilution), Nrf2 (1:2000 dilution), HO-1 (1:1000 dilution) and *β*-actin (1:1000 dilution) primary antibodies at 4 °C overnight, followed by being incubated with relevant secondary antibodies (1:5000 dilutions) for 2 h at room temperature. Protein blots were visualized by chemiluminescence in the dark.

EIU Model and Treatment

Animals (C57BL/6 mice, male, 6–8 weeks) were purchased from Shanghai SLAC Laboratory Animal Co., Ltd. All animal experiments in this study complied with the ARVO Statement for the Use of Animals in Ophthalmic and Vision Research were approved by the Zhejiang University Administration on Laboratory Animal Care.

According to the previous study,[37] the EIU mouse model was induced by the intravitreal injection of LPS (100 ng per eye) using a 30 G insulin syringe. After the intravitreal injection of LPS, mice were randomly divided into three groups and treated with PBS, EC (29.2 μg/mL), P-HPEC (with an equivalent EC concentration). The treatment for each group was performed at 3, 6, and 24 h after EIU induction by intravitreal injection. Then, slit-lamp examinations were performed to evaluate the inflammatory severity under systemic anesthesia. The clinical scores of EIU were graded according to the established method.[37]

RESULTS AND DISCUSSION

Synthesis and Characterization of Macromolecular EC Prodrug

4-(Hydroxymethyl) phenylboronic acid ethyl caffeate ester (HPEC) was synthesized at first by the reaction between EC and 4-hydroxymethyl phenylboric acid. Unlike traditional ways including tedious steps to deprotect the pinacol ester of boric acid, the direct esterification was achieved at 100 °C with consistent removal of moisture in this research. The successful synthesis of HPEC was verified by ^{1}H-NMR (Fig. S1 in the electronic supplementary information, ESI). Secondly, the ring-opening of *γ*-benzyl L-glutamic-NCA (BLG-NCA) was initiated *via* methoxypolyethylene glycol amine (MW=2000) to synthesize the polymer PEG-PBLG (Fig. 1A). The grafting benzyloxycarbonyl (Cbz) groups in PEG-PBLG were replaced with ethanolamine to get hydroxyl functionalized polymer P-OH. The polymerization and post-modification described above were supported by gel permeation chromatography (GPC) and ^{1}H-NMR (Fig. 2a, Figs. S3 and S4 in ESI). The degree of polymerization (DP) of the polypeptide block was about 30 as calculated from ^{1}H-NMR, and the polydispersity index (PDI) of polymer was as narrow as 1.04 (P-OH) or 1.05 (PEG-PBLG). Thereafter, 1,1'-carbonyldiimidazole (CDI) was used to activate hydroxyl groups, which reacted with HPEC later to obtain the prodrug P-HPEC. Besides ^{1}H-NMR, the UV-Vis spectra of prepared prodrug and its precursors were recorded to demonstrate the drug-loading pattern (Figs. 1B and 2b). Compared with the backbone P-OH, the additional absorption around 330 nm of P-HPEC was ascribed to loaded EC, and the loading efficiency was calculated as 21.6%, which agreed well with the structure inferred from ^{1}H-NMR.

Thereafter, the ROS-responsive and scavenging abilities were further investigated. To demonstrate the drug release behavior, 1 mL of solution of P-HPEC in PBS containing 1 mmol/L H_2O_2 was incubated at 37 °C in a dialysis membrane (MWCO 1000 Da)-sealed chamber, and the released drug molecules were effused into peripheric buffer and used for calculation. At the beginning of the ROS stimulation, the releasing percent bursts into 88.5% in the first 4 h and gradually accumulates to 92.1% after 24 h. In contrast, only 10.8% of loading drugs release after 24 h if P-HPEC was incubated in the absence of H_2O_2 (Fig. 2c). The antioxidant capability of P-HPEC was then tested by incubating with 100 μmol/L DPPH radical. As shown in Fig. 2(d), P-HPEC shows a concentration-dependent DPPH scavenging ability, and DPPH was nearly completely cleared at an EC equivalent concentration of 7.5 μg/mL. Both the ROS-responsive and scavenging capability of P-HPEC solidified our design and guaranteed the anti-inflammation outcomes by ROS depletion.

Rescuing Capacity of P-HPEC against Oxidative Stress on L929 and HCEC

Since excessive ROS generated during inflammation can destroy lipids, proteins and DNA, resulting in serious damage to cells, the rescuing effect of antioxidative P-HPEC was then evaluated using L929 and HCEC.

The internalization of P-HPEC by cells is the first step for ROS depletion. Therefore, Rhodamine B labelled P-HPEC was synthesized to investigate the cell uptake behavior. The uptake of P-HPEC by L929 cells was detected by fluorescence microscope. As can be seen from Fig. 3(a), the intracellular red fluorescence of Rhodamine B increases with the prolongation of incubation time, indicating that P-HPEC could be effectively internalized by L929.

In order to exclude the possibility of cytotoxicity of P-HPEC after cell uptake, the cell viability of L929 and HCEC after treated with P-HPEC was evaluated by CCK-8 (Figs. 3b and 3c). The experimental results suggested that P-HPEC exhibited minimal cytotoxicity towards L929 and HCEC. The cell viability was higher than 90% even at the highest concentration of P-HPEC (15 μg/mL EC equiv.). The dose of P-HPEC used in subsequent cell experiments was at an EC equivalent concentra-

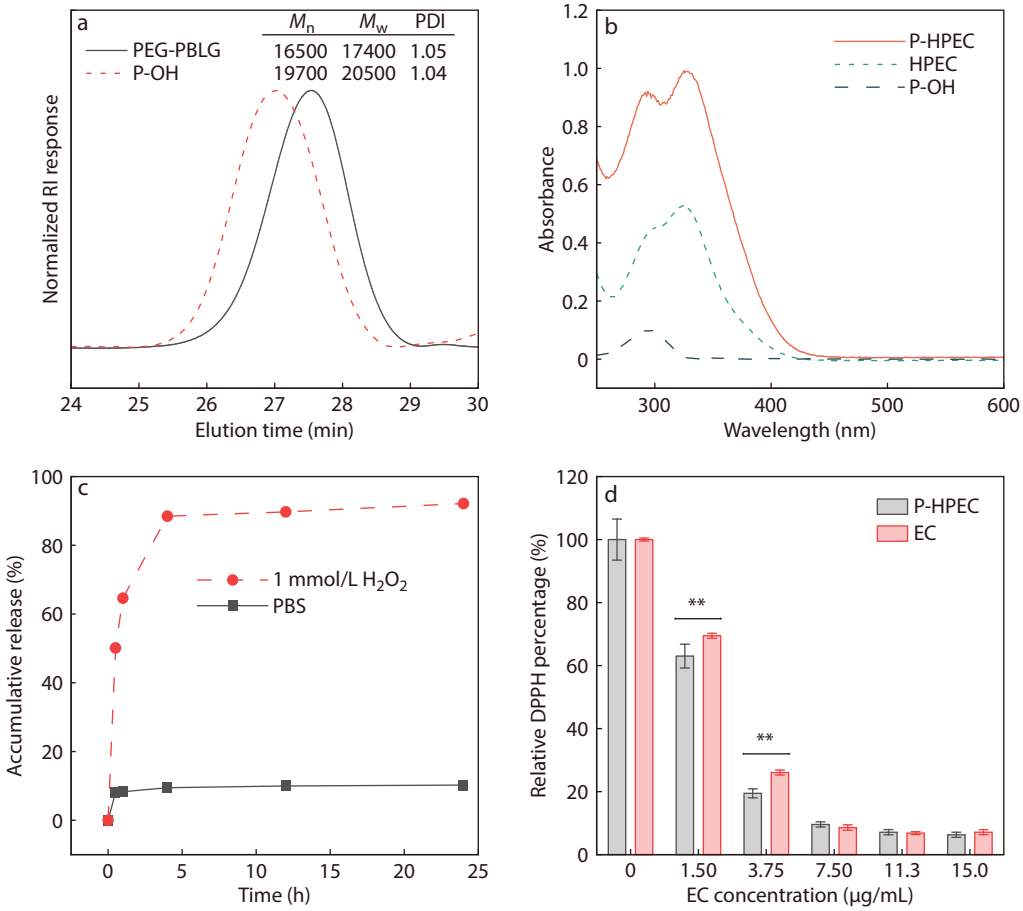

Fig. 2 Characterization of macromolecular EC prodrug P-HPEC. (a) GPC chromatogram of PEG-PBLG and P-OH; (b) UV-Vis spectra of P-OH, HPEC and P-HPEC; (c) *In vitro* release of P-HPEC in PBS (pH=7.4) and PBS (pH=7.4) containing 1 mmol/L H_2O_2; (d) Elimination of DPPH radical by P-HPEC and EC. Date are expressed as mean±s.d., n=3, and $^{**}p$<0.01 (Student's t-test).

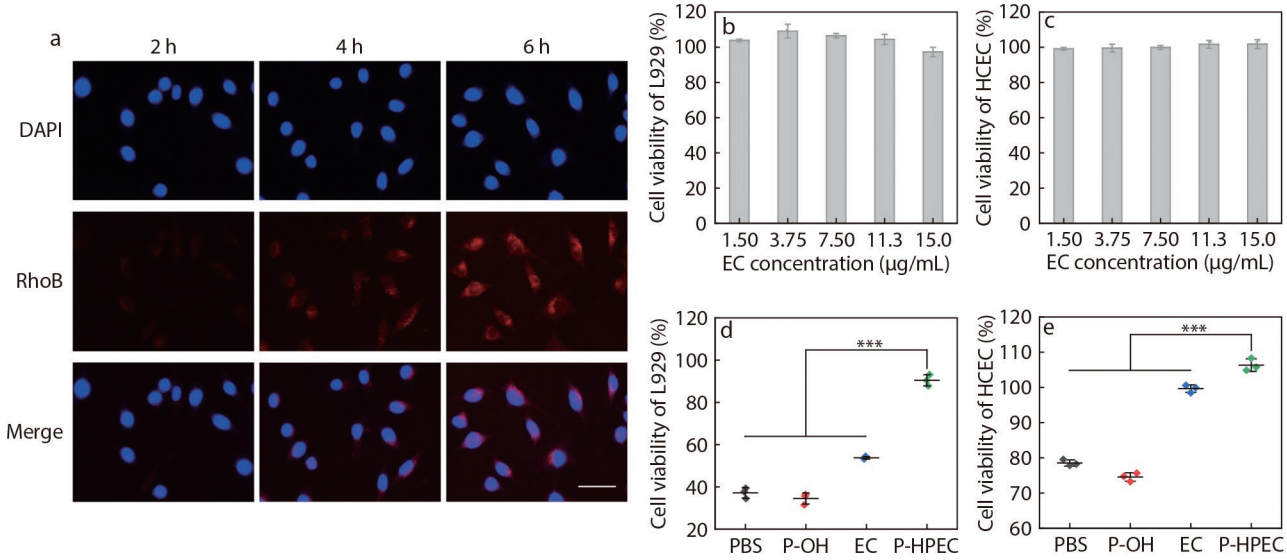

Fig. 3 Rescuing capacity of P-HPEC against oxidative stress on L929 and HCEC. (a) Images captured by fluorescence microscopy of the internalization of Rhodamine B labelled P-HPEC by L929 at different time points. Scale bar, 50μm. Cytotoxicities of P-HPEC against L929 (b) and HCEC (c); Cell viability of L929 (d) and HCEC (e) treated with H_2O_2 and simultaneously incubated with PBS, EC (7.50 μg/mL), P-HPEC (with an equivalent EC concentration) or P-OH (with an equivalent polymer backbone concentration), respectively. Date are expressed as mean±s.d., n=3, and $^{***}p$<0.001 (one-way ANOVA).

https://doi.org/10.1007/s10118-022-2798-x

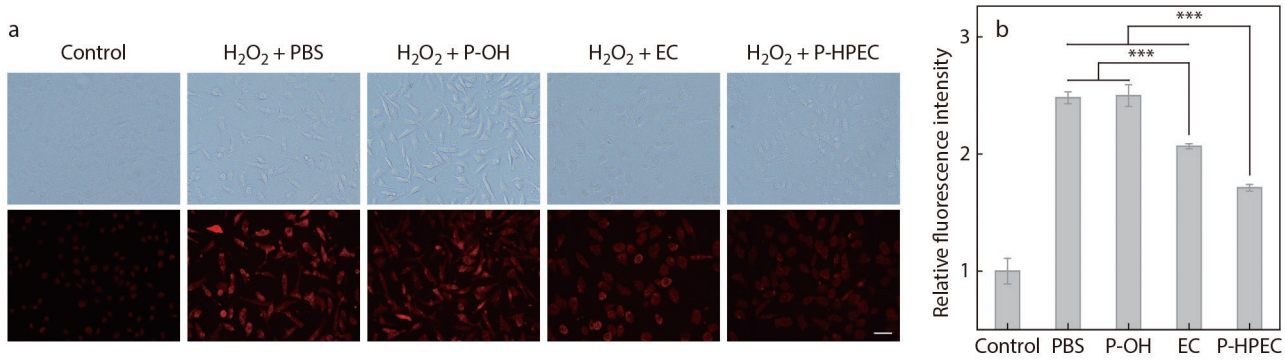

Fig. 4 Fluorescent images (a) and relative fluorescence intensity analysis (b) of intracellular ROS. L929 cells were treated with H_2O_2 and simultaneously incubated with PBS, EC (7.50 μg/mL), P-HPEC (with an equivalent EC concentration) or P-OH (with an equivalent polymer backbone concentration), respectively. Scale bar, 50 μm.

tion of 7.5 μg/mL, which indicated the excellent biosafety of P-HPEC.

It has been proven that P-HPEC could be internalized by cells without obvious cytotoxicity. Next, it is necessary to investigate whether P-HPEC can play its antioxidative function intracellularly. In this study, H_2O_2 was used to simulate the oxidative stress environment of L929 and HCEC (Fig. S5 in ESI). H_2O_2 treated L929 and HCEC were simultaneously incubated with PBS, EC, empty carrier P-OH, or P-HPEC to evaluate their rescuing capacity against oxidative stress. As shown in Figs. 3(d) and 3(e), H_2O_2 shows obvious cytotoxicity due to the significantly increased oxidative stress. P-OH has almost no protective effect against oxidative stress since it shows no antioxidative capability. EC does have some rescuing effects due to its intrinsic antioxidative capability. Surprisingly, P-HPEC exhibits much better protective effect than free EC with significant difference, which might be ascribed to the dual antioxidative capability of released EC and HBA. P-HPEC had significant cell rescuing capacity and could effectively inhibit oxidative stress-induced cell apoptosis.

To further explore the potential reasons of the rescuing capacity of P-HPEC, intracellular ROS level was investigated by fluorescent imaging after H_2O_2 treated L929 cells were simultaneously incubated with PBS, EC, P-OH and P-HPEC (Fig. 4). It could be intuitively observed that the red fluorescence of ROS was significantly enhanced after H_2O_2 incubation. Compared with the H_2O_2 treated group, EC and P-HPEC could effectively reduce intracellular ROS level. The ROS fluorescence of the P-HPEC group is lower than EC group, suggesting that P-HPEC has a stronger ROS scavenging activity than EC.

As immunomodulators, cytokines are proteins produced by immune cells that can participate in the process of biological immune response, among which, TNF-*α* is a potent pro-inflammatory factor and plays an important role in inflammatory response.[38,39] Therefore, the determination of intracellular TNF-*α* content can indicate the degree of inflammation. Western blot analysis was used to demonstrate the content of TNF-*α* in L929 induced by H_2O_2 and simultaneous treatment with PBS, P-OH, EC, or P-HPEC. As shown in Fig. 5, the expression of TNF-*α* in L929 cells increases significantly after being treated with H_2O_2, which implied serious inflammatory response induced by H_2O_2. EC cannot effectively inhibit the expression of TNF-*α* release. In sharp contrast, P-HPEC is very effective in inhibiting the expression of pro-inflammatory cytokine TNF-*α*, which implies that P-HPEC is an ideal candidate in inhibiting ROS-induced inflammatory response. In addition, Nrf2-HO1 signalling pathway, as a key signal pathway of endogenous antioxidant stress, can regulate the expression of antioxidant protein genes and induce the upregulation of HO-1 (heme oxygenase-1) by activating Nrf2 (nuclear factor erythroid-2 related factor 2), playing a key role in intracellular antioxidant stress.[40,41] The expression of Nrf2 and HO-1 in L929 cells was also greatly down-regulated after H_2O_2 treated L929 cells were incubated with P-HPEC at the same time, which was consistent with the trend of TNF-*α*. These results indicated that P-HPEC could effectively alleviate oxidative stress and inhibit inflammatory response, leading to excellent cell rescuing capacity.

Alleviation of Uveitis *In vivo*

To examine the *in vivo* therapeutic efficacy on endotoxin-induced uveitis (EIU) model, we compared the therapeutic effects of P-HPEC with PBS and EC (Fig. 6a). As shown in Fig. 6(b),

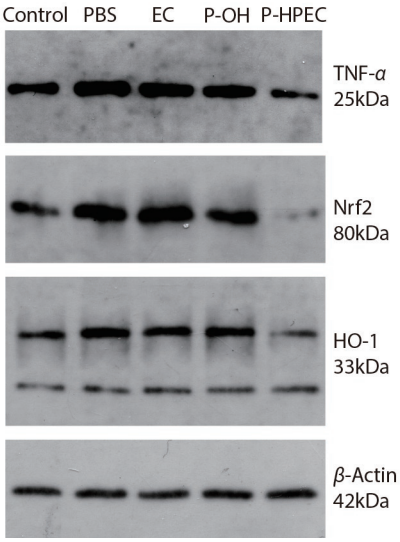

Fig. 5 Western bloting analysis of TNF-*α*, Nrf2, and HO-1 in L929 cells. L929 cells were treated with H_2O_2 and simultaneously incubated with PBS, EC (7.50 μg/mL), P-HPEC (with an equivalent EC concentration) or P-OH (with an equivalent polymer backbone concentration), respectively.

https://doi.org/10.1007/s10118-022-2798-x

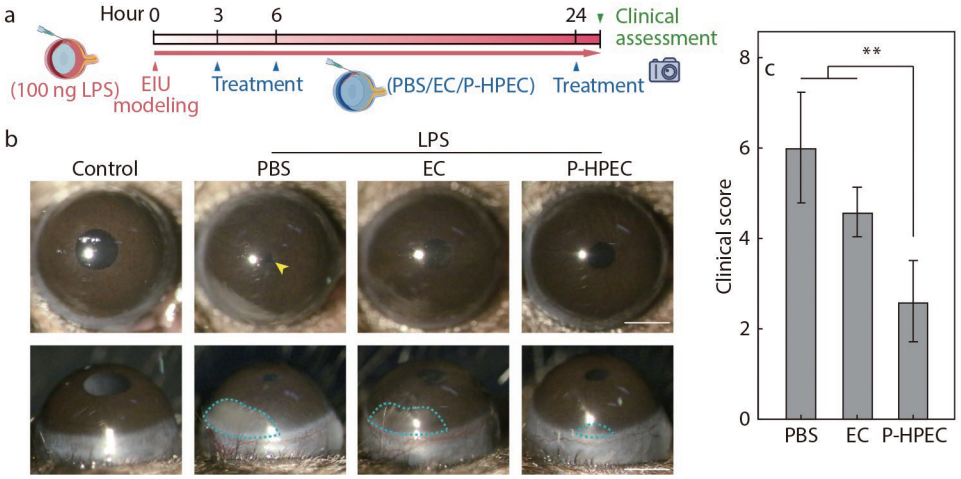

Fig. 6 P-HPEC exhibits the potent therapeutic efficacy in EIU mouse model. (a) Schematic diagram of EIU induction, treatment with PBS, EC (29.2 μg/mL) and P-HPEC (with an equivalent EC concentration), and observation in mice; (b) Representative photographs anterior ocular segment of each group. Arrow indicates the pupil synechiae. Blue dashed line indicates the area of purulent exudate. Scale bar, 1 mm. (c) Clinical score of inflammatory severity from each group. Date are expressed as mean±s.d., n=5, and $^{**}p<0.01$ (one-way ANOVA).

the intravitreal injection of LPS stimulates typical clinical signs of anterior uveitis including pupil synechiae, exudate in anterior chamber, and hypopyon after 24 h. The treatment of EC partially relieves the inflammatory response and the low therapeutic performance of EC might be attributed to its very low water solubility. However, P-HPEC could remarkably alleviate these inflammatory responses. This result was consistent with the clinical score, in which P-HPEC-treated group was significantly lower than those of PBS group and EC group (Fig. 6c).

CONCLUSIONS

In summary, we developed a macromolecular EC prodrug P-HPEC that conjugated EC to a water-soluble and biocompatible macromolecular chain of polyglutamic acid through a phenylboronic acid ester linkage. The macromolecular prodrug was sensitive under ROS stimulation and produced two kinds of antioxidants, EC and HBA, with dual ROS scavenging capability. P-HPEC was able to effectively inhibit cell apoptosis induced by H_2O_2 in L929 and HCEC, implying excellent cell rescuing capacity. Meanwhile, P-HPEC was effective in depleting intracellular ROS and inhibiting the expression of pro-inflammatory cytokine TNF-α. In addition, the *in vivo* endotoxin-induced uveitis (EIU) model indicated that P-HPEC could effectively protect mice from LPS-induced uveitis injury. Overall, this study provided a promising therapeutic strategy for the treatment of uveitis, which was also instructive in the alleviation of other ROS related diseases.

NOTES

The authors declare no competing financial interest.

Electronic Supplementary Information

Electronic supplementary information (ESI) is available free of charge in the online version of this article at http://doi.org/10.1007/s10118-022-2798-x.

ACKNOWLEDGMENTS

This work was financially supported by National Key Research and Development Project (No. 2020YFE0204400).

REFERENCES

1 Lee, R. W.; Nicholson, L. B.; Sen, H. N.; Chan, C. C.; Wei, L.; Nussenblatt, R. B.; Dick, A. D. Autoimmune and autoinflammatory mechanisms in uveitis. *Semin. Immunopathol.* **2014**, *36*, 581–594.
2 Li, W.; He, B.; Dai, W.; Zhang, Q.; Liu, Y. Evaluations of therapeutic efficacy of intravitreal injected polylactic-glycolic acid microspheres loaded with triamcinolone acetonide on a rabbit model of uveitis. *Int. Ophthalmol.* **2014**, *34*, 465–476.
3 Mahran, A.; Ismail, S.; Allam, A. A. Development of triamcinolone acetonide-loaded microemulsion as a prospective ophthalmic delivery system for treatment of uveitis: *in vitro* and *in vivo* evaluation. *Pharmaceutics* **2021**, *13*, 444.
4 Shome, A.; Mugisho, O. O.; Niederer, R. L.; Rupenthal, I. D. Blocking the inflammasome: a novel approach to treat uveitis. *Drug Discov. Today* **2021**, *26*, 2839–2857.
5 Garg, V.; Nirmal, J.; Riadi, Y.; Kesharwani, P.; Kohli, K.; Jain, G. K. Amelioration of endotoxin-induced uveitis in rabbit by topical administration of tacrolimus proglycosome nano-vesicles. *J. Pharm. Sci.* **2021**, *110*, 871–875.
6 Ung, L.; Pattamatta, U.; Carnt, N.; Wilkinson-Berka, J. L.; Liew, G.; White, A. J. R. Oxidative stress and reactive oxygen species: a review of their role in ocular disease. *Clin. Sci.* **2017**, *131*, 2865–2883.
7 Xu, Q. Y.; Zhang, J.; Qin, T. Y.; Bao, J. Y.; Dong, H. T.; Zhou, X. R.; Hou, S. P.; Mao, L. M. The role of the inflammasomes in the pathogenesis of uveitis. *Exp. Eye Res.* **2021**, *208*, 108618.
8 Zhou, R.; Tardivel, A.; Thorens, B.; Choi, I.; Tschopp, J. Thioredoxin-interacting protein links oxidative stress to inflammasome activation. *Nat. Immunol.* **2010**, *11*, 136–140.
9 Ahmad, A.; Ahsan, H. Biomarkers of inflammation and oxidative stress in ophthalmic disorders. *J. Immunoassay Immunochem.* **2020**, *41*, 257–271.

10 Choulaki, C.; Papadaki, G.; Repa, A.; Kampouraki, E.; Kambas, K.; Ritis, K.; Bertsias, G.; Boumpas, D. T.; Sidiropoulos, P. Enhanced activity of NLRP3 inflammasome in peripheral blood cells of patients with active rheumatoid arthritis. *Arthritis Res. Ther.* **2015**, *17*, 257.
11 Ou, A. T.; Zhang, J. X.; Fang, Y. F.; Wang, R.; Tang, X. P.; Zhao, P. F.; Zhao, Y. G.; Zhang, M.; Huang, Y. Z. Disulfiram-loaded lactoferrin nanoparticles for treating inflammatory diseases. *Acta Pharmacol. Sin.* **2021**, *42*, 1913–1920.
12 Mishra, S. R.; Mahapatra, K. K.; Behera, B. P.; Patra, S.; Bhol, C. S.; Panigrahi, D. P.; Praharaj, P. P.; Singh, A.; Patil, S.; Dhiman, R.; Bhutia, S. K. Mitochondrial dysfunction as a driver of NLRP3 inflammasome activation and its modulation through mitophagy for potential therapeutics. *Int. J. Biochem. Cell Biol.* **2021**, *136*, 106013.
13 van der Vliet, A.; Janssen-Heininger, Y. M. Hydrogen peroxide as a damage signal in tissue injury and inflammation: murderer, mediator, or messenger. *J. Cell. Biochem.* **2014**, *115*, 427–435.
14 Halliwell, B. Biochemistry of oxidative stress. *Biochem. Soc. Trans.* **2007**, *35*, 1147–1150.
15 Yadav, U. C. S.; Kalariya, N. M.; Ramana, K. V. Emerging role of antioxidants in the protection of uveitis complications. *Curr. Med. Chem.* **2011**, *18*, 931–942.
16 Li, Z.; Li, H.; Zhang, J.; Liu, X.; Gu, Z.; Li, Y. Ultrasmall nanoparticle ROS scavengers based on polyhedral oligomeric silsesquioxanes. *Chinese J. Polym. Sci.* **2020**, *38*, 1149–1156.
17 Granata, G.; Paterniti, I.; Geraci, C.; Cunsolo, F.; Esposito, E.; Cordaro, M.; Blanco, A. R.; Cuzzocrea, S.; Consoli, G. M. L. Potential eye drop based on a calix[4]arene nanoassembly for curcumin delivery: enhanced drug solubility, stability, and anti-inflammatory effect. *Mol. Pharm.* **2017**, *14*, 1610–1622.
18 Deng, J.; Lin, D. Q.; Ding, X. Y.; Wang, Y.; Hu, Y. H.; Shi, H.; Chen, L.; Chu, B. Y.; Lei, L.; Wen, C. M.; Wang, J. Q.; Qian, Z. Y.; Li, X. Y. Multifunctional supramolecular filament hydrogel boosts anti-inflammatory efficacy *in vitro* and *in vivo*. *Adv. Funct. Mater.* **2022**, *32*, 2109173.
19 Masuda, T.; Yamada, K.; Akiyama, J.; Someya, T.; Odaka, Y.; Takeda, Y.; Tori, M.; Nakashima, K.; Maekawa, T.; Sone, Y. Antioxidation mechanism studies of caffeic acid: identification of antioxidation products of methyl caffeate from lipid oxidation. *J. Agric. Food Chem.* **2008**, *56*, 5947–5952.
20 Chiang, Y. M.; Lo, C. P.; Chen, Y. P.; Wang, S. Y.; Yang, N. S.; Kuo, Y. H.; Shyur, L. F. Ethyl caffeate suppresses NF-kappaB activation and its downstream inflammatory mediators, iNOS, COX-2, and PGE2 *in vitro* or in mouse skin. *Br. J. Pharmacol.* **2005**, *146*, 352–363.
21 Mao, Y. W.; Tseng, H. W.; Liang, W. L.; Chen, I. S.; Chen, S. T.; Lee, M. H. Anti-inflammatory and free radial scavenging activities of the constituents isolated from Machilus zuihoensis. *Molecules* **2011**, *16*, 9451–9466.
22 Kularatne, R. N.; Bulumulla, C.; Catchpole, T.; Takacs, A.; Christie, A.; Stefan, M. C.; Csaky, K. G. Protection of human retinal pigment epithelial cells from oxidative damage using cysteine prodrugs. *Free Radic. Biol. Med.* **2020**, *152*, 386–394.
23 Muangnoi, C.; Phumsuay, R.; Jongjitphisut, N.; Waikasikorn, P.; Sangsawat, M.; Rashatasakhon, P.; Paraoan, L.; Rojsitthisak, P. Protective effects of a lutein ester prodrug, lutein diglutaric acid, against H_2O_2-induced oxidative stress in human retinal pigment epithelial cells. *Int. J. Mol. Sci.* **2021**, *22*, 4722.
24 Zhang, C.; Lu, H. Helical nonfouling polypeptides for biomedical applications. *Chinese J. Polym. Sci.* **2022**, *40*, 433–446.
25 Song, Z.; Han, Z.; Lv, S.; Chen, C.; Chen, L.; Yin, L.; Cheng, J. Synthetic polypeptides: from polymer design to supramolecular assembly and biomedical application. *Chem. Soc. Rev.* **2017**, *46*, 6570–6599.
26 Liu, Y.; Li, D.; Ding, J.; Chen, X. Controlled synthesis of polypeptides. *Chin. Chem. Lett.* **2020**, *31*, 3001–3014.
27 Ren, J.; Shu, X.; Wang, Y.; Wang, D.; Wu, G.; Zhang, X.; Jin, Q.; Liu, J.; Wu, Z.; Xu, Z.; Li, C. Z.; Li, H. Key progresses of MOE key laboratory of macromolecular synthesis and functionalization in 2020. *Chin. Chem. Lett.* **2022**, *33*, 1650–1658.
28 Xiong, R.; Xu, R. X.; Huang, C.; De Smedt, S.; Braeckmans, K. Stimuli-responsive nanobubbles for biomedical applications. *Chem. Soc. Rev.* **2021**, *50*, 5746–5776.
29 Han, H.; Hou, Y.; Chen, X.; Zhang, P.; Kang, M.; Jin, Q.; Ji, J.; Gao, M. Metformin-induced stromal depletion to enhance the penetration of gemcitabine-loaded magnetic nanoparticles for pancreatic cancer targeted therapy. *J. Am. Chem. Soc.* **2020**, *142*, 4944–4954.
30 Gao, Y.; Wang, J.; Chai, M.; Li, X.; Deng, Y.; Jin, Q.; Ji, J. Size and charge adaptive clustered nanoparticles targeting the biofilm microenvironment for chronic lung infection management. *ACS Nano* **2020**, *14*, 5686–5699.
31 Deng, Y.; Wang, Y.; Jia, F.; Liu, W.; Zhou, D.; Jin, Q.; Ji, J. Tailoring supramolecular prodrug nanoassemblies for reactive nitrogen species-potentiated chemotherapy of liver cancer. *ACS Nano* **2021**, *15*, 8663–8675.
32 Tao, W.; He, Z. ROS-responsive drug delivery systems for biomedical applications. *Asian J. Pharm. Sci.* **2018**, *13*, 101–112.
33 Xu, Q.; He, C.; Xiao, C.; Chen, X. Reactive oxygen species (ROS) responsive polymers for biomedical applications. *Macromol. Biosci.* **2016**, *16*, 635–646.
34 Broaders, K. E.; Grandhe, S.; Frechet, J. M. A biocompatible oxidation-triggered carrier polymer with potential in therapeutics. *J. Am. Chem. Soc.* **2011**, *133*, 756–758.
35 Liu, D.; Cornel, E. J.; Du, J. Renoprotective angiographic polymersomes. *Adv. Funct. Mater.* **2020**, *31*, 2007330.
36 Tian, Z. Y.; Zhang, Z.; Wang, S.; Lu, H. A moisture-tolerant route to unprotected *α*/*β*-amino acid *N*-carboxyanhydrides and facile synthesis of hyperbranched polypeptides. *Nat. Commun.* **2021**, *12*, 5810.
37 Qiu, Y.; Shil, P. K.; Zhu, P.; Yang, H.; Verma, A.; Lei, B.; Li, Q. Angiotensin-converting enzyme 2 (ACE2) activator diminazene aceturate ameliorates endotoxin-induced uveitis in mice. *Invest. Ophthalmol. Vis. Sci.* **2014**, *55*, 3809–3818.
38 Yang, Z.; Min, Z.; Yu, B. Reactive oxygen species and immune regulation. *Int. Rev. Immunol.* **2020**, *39*, 292–298.
39 Weinstein, J. E.; Pepple, K. L. Cytokines in uveitis. *Curr. Opin. Ophthalmol.* **2018**, *29*, 267–274.
40 Yuan, H.; Xu, Y.; Luo, Y.; Wang, N. X.; Xiao, J. H. Role of Nrf2 in cell senescence regulation. *Mol. Cell. Biochem.* **2021**, *476*, 247–259.
41 Bao, M.; Liang, M.; Sun, X.; Mohyuddin, S. G.; Chen, S.; Wen, J.; Yong, Y.; Ma, X.; Yu, Z.; Ju, X.; Liu, X. Baicalin alleviates LPS-induced oxidative stress *via* NF-kappaB and Nrf2-HO1 signaling pathways in IPEC-J2 cells. *Front. Vet. Sci.* **2021**, *8*, 808233.

https://doi.org/10.1007/s10118-022-2798-x